A R C H I V E O F M E C H A N I C A L E N G I N E E R I N G

VOL. LXIII 2016 Number 3

DOI: 10.1515/meceng-2016-0024

Key words: thermal shock, low cycle fatigue, crack growth under thermal shocks, adaptation to thermal shocks, leak but not burst

JAKUB PAWLICKI [1], *PIOTR MAREK* [1], *JANISŁAW ZWOLIŃSKI* [1]

FINITE ELEMENT MODELING OF MATERIAL FATIGUE AND CRACKING PROBLEMS FOR STEAM POWER SYSTEM HP DEVICES EXPOSED TO THERMAL SHOCKS

The paper presents a detailed analysis of the material damaging process due to low-cycle fatigue and subsequent crack growth under thermal shocks and high pressure. Finite Element Method (FEM) model of a high pressure (HP) by-pass valve body and a steam turbine rotor shaft (used in a coal power plant) is presented. The main damaging factor in both cases is fatigue due to cycles of rapid temperature changes. The crack initiation, occurring at a relatively low number of load cycles, depends on alternating or alternating-incremental changes in plastic strains. The crack propagation is determined by the classic fracture mechanics, based on finite element models and the most dangerous case of brittle fracture. This example shows the adaptation of the structure to work in the ultimate conditions of high pressure, thermal shocks and cracking.

1. Introduction

Breakdowns and structural damage to the elements of mechanical devices, where high energy of gaseous media (tanks and pressure system components) and mechanical energy (rotating machinery parts) are concentrated, usually lead to serious consequences. Detailed engineering failure analysis often requires FEM modeling combined with experimental data gathering [1]. Atypical failure mechanism is often the destruction of material through the fracture. The process of crack initiation and its subsequent development is a complex issue, subject to the influence of a wide range of factors. Among the most important factors are the current mechanical properties of the material, depending on the type and grade, the method of treatment (heat, mechanical, surface), the

[1] *Institute of Aeronautics and Applied Mechanics, Warsaw University of Technology; Emails: kubap@autograf.pl, pmarek@meil.pw.edu.pl, jzwolin@meil.pw.edu.pl*

presence of defects in material, the mechanical and thermal loading conditions, as well as corrosion and erosion of the material. Generally, these factors can be divided into two groups: I – internal material properties that determine its condition; and II – external, environmental factors, including loads, corrosion and erosion. The superposition of these factors in each individual case can create unique conditions resulting in degradation of material and consequently the structural damage due to cracking. Crack initiation due to fatigue occurs in the material subjected to a cyclically-variable load, where the intensity of fatigue depends on the amplitude of local changes in strain (low cycle fatigue) and the stress state (high cycle fatigue). It is essential to distinguish static mechanical load, related to the impact of pressure or body forces, that do not depend significantly on system deformation (or increase with deformation), from kinematic extortion (e.g. thermal expansion, bolts preload, etc.), which is usually less dangerous and often disappears as a result of permanent deformation of the structure. The redistribution of stresses due to plastic deformation of the structure or other forms of non-linear behavior of the material (creep, cracking, buckling) after a finite number of initial cycles of load, particularly in the kinematic and complex (simultaneous static and kinematic) loading conditions, often allows for a safe, long-term operation of the construction as a result of adaptation of the structure to a given load scheme (cycles). An example of such adaptation may be the elastic-plastic structure shakedown in simple and complex load programs, when plastic deformation occurs in the initial cycles of load and creates a self-equilibrated state of residual stresses. If the superposition of these residual stresses with the stress field in subsequent load cycles allows the structure to operate in purely elastic manner, with no change in plastic deformation, then the shakedown occurs according to the Melan theorem [2]. Otherwise, the structure becomes damaged in a finite number of cycles of incremental or alternating plastic deformation [3]. Similarly, in the case of fracture the structure may adapt to the changing conditions of load or may fail due to the dynamics of the process of cracking. A particularly interesting cases seem to be structures, which after the crack initiation due to low cyclic fatigue, as a result of subsequent crack propagation, adapt to operate at the next cycle of the same variable loads without further damage. This is most feasible for metals exposed to repeated thermal cold shocks as the fatigue limit for these materials is about an order of magnitude less than their fracture toughness [4] and temperature gradient decreases into the depths of the solid.

2. Thermal shocks

The essence of the process of fatigue is the degradation of the material properties during cyclic load changes. The most common cause of fatigue in

real structures are complex loads, when their static and kinematic forms coexist. If all components of loads vary in time in proportion to a single parameter, such a load is called the simple one, and the shakedown analysis of elastic-perfectly-plastic structure can be limited to certain conditions on the envelope of loads states [5]. Otherwise, it is necessary to trace the history of loads of the structure. A common form of time-varying loads are cyclic temperature changes. They cause a large variation of the stress field due to non-uniform thermal expansion of individual parts of the structure. This is particularly dangerous in the case of thermal shocks when temperature changes are abrupt [6].

To assess the state of stress and strain in such situations it is necessary to find the transient temperature field $T(x, y, z, t)$ at time t of a heat shock on the basis of heat conduction equation:

$$\frac{\partial}{\partial x}\left(k_x \frac{\partial T}{\partial x}\right) + \frac{\partial}{\partial y}\left(k_y \frac{\partial T}{\partial y}\right) + \frac{\partial}{\partial z}\left(k_z \frac{\partial T}{\partial z}\right) + q_v(x, y, z, t) = c\rho \frac{\partial T}{\partial t}, \tag{1}$$

where:
k_x, k_y, k_z – thermal conductivity coefficients, W/(m K),
q_v – heat source, W/m^3,
c – specific heat, J/(kgK),
ρ – density, kg/m^3.

For a homogeneous, thermally isotropic body with thermal diffusivity $a = k/c\rho$ and no internal heat sources it can be simplified to the form:

$$\operatorname{div}(\operatorname{grad} T) = \frac{1}{a}\frac{\partial T}{\partial t} \qquad \text{or} \qquad \nabla^2 T = \frac{1}{a}\frac{\partial T}{\partial t}. \tag{2}$$

Technically important case is a shock, or heat blow, caused by a sudden change in the conditions of convective heat transfer specified by coefficient α, W/(m^{2}K), between the liquid at the temperature T_p and the body at the temperature T_c where the heat flux density on its surface is:

$$q = \alpha(T_p - T_c). \tag{3}$$

The components of the strain ε_{ij} and stress σ_{ij} tensor of elastic body with Kirchhoff's modulus G and Poisson's ratio ν, taking into account the components resulting from the temperature increase of the ΔT, can be expressed by equations:

$$\varepsilon_{ij} = \frac{1}{2G}\left(\sigma_{ij} - \frac{\nu}{1+\nu}\delta_{ij}\sigma_{kk}\right) + \lambda \Delta T \delta_{ij} \tag{4}$$

and

$$\sigma_{ij} = 2G\left[\varepsilon_{ij} + \frac{\nu}{1-2\nu}\delta_{ij}\left(\varepsilon_{kk} - \frac{1+\nu}{\nu}\lambda\Delta T\right)\right]. \tag{5}$$

The temperature gradients in transient states, and hence the consequences of a mechanical nature, depend on the Biot number:

$$Bi = \frac{\alpha l}{k}, \tag{6}$$

which describes the relationship between the intensity of the heat exchange on the convection surface (α), and the conduction of heat into the body (k) having a characteristic thickness of l.

The destructive effects of heat shock occur for large Biot numbers, when heat transfer on the surface of the body is much more efficient than its conduction into the body. This particularly concerns fluids of high specific heat and efficient mechanism of convection (forced convection), e.g. at boiling and rapid evaporation of the liquid (when the Biot number reaches values even greater than 100). Gases generally do not cause such dramatic effects (the Biot number of 0.1–10) [7].

In the practical issues of the fatigue strength of structural components subjected to cyclic heat load, the approximate calculation methods, e.g. finite element method (FEM), are used for the evaluation of the extreme gradients of temperature and related fields of stress and strain, assuming non-stationary heat conduction and thermo-elastic-plastic deformation of the body. Additionally, the significant factors are the thermomechanical background of low cycle fatigue process and plastic strain rate, driving the material properties change. Long-term exposure to the high temperature, as well as its rapid repetitive changes, can lead to gradual material deterioration in the result of remarkable microstructure change due to creep and thermal fatigue [8]. Creep-fatigue interactions are usually complex and not fully understood yet. In order to assess the stability of the structure working in conditions of cracking, it is necessary to develop numerical models and analyze the fatigue crack initiation, and subsequent development of the cracks.

2.1. Fatigue

The fatigue is defined here as the degradation of the mechanical properties of the material under cyclically variable mechanical loads, consequently leading to its destruction. Fatigue is influenced by the design (defined by the type and structure of the material, applied treatment, shape, support conditions) and established cycle parameters, which may vary in nature and course depending on the number of cycles in which the failure occurs and the deformation state.

For the low-cycle fatigue destruction processes running at a low number of cycles ($10 \div 10^4$) and high amplitude loading, the law of Manson-Coffin is used, combining the number of cycles leading to destruction N_f with an amplitude

of plastic deformation $\Delta\varepsilon_{pl}$:

$$N_f^k \Delta\varepsilon_{pl} = C, \tag{7}$$

where k and C are material constants, and C represents the reduction of the specimen Z (initial cross-section A_0 to the cross-section of the neck A_k) at the point of breaking in the tensile test and equals a half of the actual elongation of the material ε_{rz}:

$$C = \frac{1}{2} \ln \frac{A_0}{A_K} = \frac{\varepsilon_{rz}}{2}. \tag{8}$$

The course of high cycle fatigue ($N > 10^5$ cycles) within the limits established for the cycle of stress (for given mean value and amplitude) can be determined from the classic form of the Wohler's graph based on available results of fatigue tests. At elevated temperatures, the fatigue strength is usually reduced, and the possibility of permanent fatigue strength usually disappears. In the transitional range of $N = 10^4 \div 10^5$ cycles, the influences from each of the models may be present. In the case of thermal shocks, the mechanical fatigue process is accompanied by the thermal fatigue of the material, associated with changes in the structure and properties of the material (e.g. phase transitions). Interaction between mechanical and thermal factors in the fatigue process are much simpler in an isotonic process, when the cycles of mechanical loads are correlated with the changes in temperature. Thermal fatigue occurring on a small number of cycles and, in particular, at high temperatures, is the result of the cumulative effects of processes such as plastic deformation, creep, stress relaxation, an increase in the volume of material as a result of the mass development of micro cracks and voids. Numerous studies [9] confirms the relevance and applicability of the law of Manson-Coffin to the issues of thermal and thermo-mechanical fatigue, taking into consideration the updated material properties (k, C). The important factors are also the course and time of cooling and heating cycles (due to creep) and corrosion that progresses intensively at high temperatures. The effects of these multi-parametric interactions may be difficult to estimate and accurate prediction of fatigue properties requires advanced materials testing [6, 9, 10]. A significant problem in real cases of fatigue analysis is to clearly define all the details of heat exchange and courses of thermal and mechanical cycles, as well as the complete material and structural properties across the range of temperatures and strain fields. In such cases, assessing the safety and durability of structures often requires a number of the most unfavorable model estimation methods of estimating the limit load cycles, and the other parameters of the process of fatigue, followed by investigation of the mechanics of fatigue crack growth.

2.2. Fracture

The process of fracture (the crack growth) is driven by the increase of the characteristic dimension of the crack and depends on the type of material and its properties, that in the case of thermal shocks may change rapidly. Fracture is initiated by the nucleation of crack and its further growth (propagation) takes place in two stages:

- Subcritical stable crack growth – crack spreads relatively slowly with increasing load,
- Critical unstable crack growth – crack spreads in an uncontrolled manner even without an increase in load.

In both analyzed cases, classic linear-elastic model of fracture mechanics is used assuming that, with the appearance of macro-cracks, the cracks propagate in the elastic deformation conditions (brittle fracture) under the first (of three) mode (kinematical scheme) of cracking, as the typical effect of thermal shocks, and the surface of the crack is perpendicular to the direction of maximum principal stress. This approach is justified by the fact that the area of plastic deformation at the crack tip is insignificant in comparison to the size of the analyzed structure. Then, the model also provides a safe (upper) estimate of the speed of cracking. Full verification of the accuracy of that assumption, based on the material study of the surface of cracks, was not possible.

The stresses field around the crack tip is characterized by the relationship:

$$\sigma_y = \frac{K_I}{\sqrt{2\pi r}} f_1(\theta); \quad \sigma_{xy} = \frac{K_{II}}{\sqrt{2\pi r}} f_2(\theta); \quad \sigma_{yz} = \frac{K_{III}}{\sqrt{2\pi r}} f_3(\theta); \tag{9}$$

where: r is the distance from the tip and $f_i(\theta$ are functions of θ angle (Fig. 1).

Stress field has a singularity $1/\sqrt{1}$ at the vertex ($r = 0$), and the stress intensity factors:K_I, K_{II}, K_{III}, refer to the three basic kinematic schemes (modes) of the crack deformation.

The development of a crack depends on the critical value of the stress intensity factor K_C, which is a material property known as fracture toughness. After reaching this value, unstable development of the crack begins.

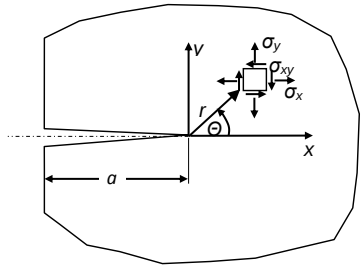

Fig. 1. The stress state in the vicinity of the crack's tip in plane stress

Stress intensity factors depend on the depth of the crack, the shape of the element, a method of loading and its level. They are to be calculated on FEM models with singular crack elements [11].

In the subcritical range it is possible to estimate the rate of crack growth per cycle of load as a function of stress intensity range according to the Erdogan--Paris equation:

$$\mathrm{d}a/\mathrm{d}N = C(\Delta K)^m, \tag{10}$$

where: $\Delta K = (1-R)K_{\max}$ and $R = K_{\min}/K_{\max}$ is the coefficient of asymmetry of the cycle.

Safe assumption of $R = 0$ for complex and variable load conditions implies $\Delta K = K_{\max} = K_I$, and the velocity of crack propagation can be calculated as:

$$\mathrm{d}a/\mathrm{d}N = C(K_I)^m. \tag{11}$$

Taking the values of C and m from the available material testing, the crack velocity can be presented as a function of the depth of the slot a.

Finally, integrating the inverse function of the speed, one obtains the relationship between the crack depth and the number of cycles given by:

$$N = \int_{a_0}^{a} \frac{1}{C\,(K_I)^m}\,\mathrm{d}a. \tag{12}$$

Scientific and engineering publishings on thermal fatigue and cracking of steam energy system elements present a theoretical material, or examination-investigation [12–16] aspects of the problem. Insight into unusual fatigue and cracking process development by finite element modeling in two application cases is the objective of this paper. All calculations presented below have been done using ANSYS system [17].

2.3. The case of the valve body

The high-pressure by-pass valves (Fig. 2) are widely used in steam power systems to reduce critical steam parameters through a decrease in the pressure by throttling and saturating steam by periodic injections of water.

The body of this steam pressure reducing valve consists of two spherical chambers of the maximum external diameter Ø560mm and the wall thickness of 32 to 66 mm. This part is forged in three dimensions of 10CrMo9-10 steel and operates at a steam pressure $p_{\text{in}} = 187$ bar and a temperature of $T_{\text{in}} = 545$°C at the inlet and pressure $p_{\text{out}} = 46$ bar and a temperature of $T_{\text{out}} = 300$°C at the outlet. Periodic injections of water at the temperature $T_w = 30$°C to the

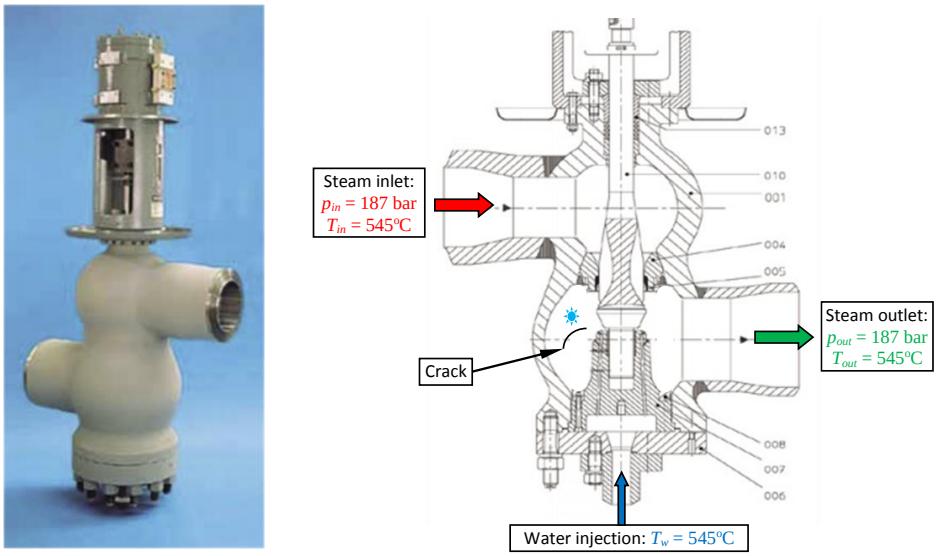

Fig. 2. The high-pressure bypass valve of steam with water injection

spherical valve chamber cause cracks on the inner surface of the body, which rapidly propagate deep into the wall. The high cost of regeneration of the valve body every 2 years prompted the user to assess the dynamics of the process of initiation and development of the cracks and possible ways to remedy the problem.

Using the finite element method, the calculations were carried out using a three-dimensional FEM model (Fig. 3) including the heat transfer and stress distribution at steady-state conditions of the valve (Fig. 4). A transient analysis of the phenomena was applied in the following three stages:

1. Determination of the time-spatial temperature fields for three-dimensional problems of transient heat transfer during thermal shock, caused

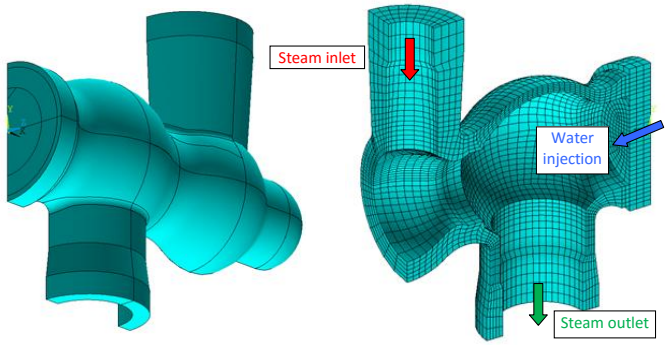

Fig. 3. FEM model of the bypass valve body with water injection

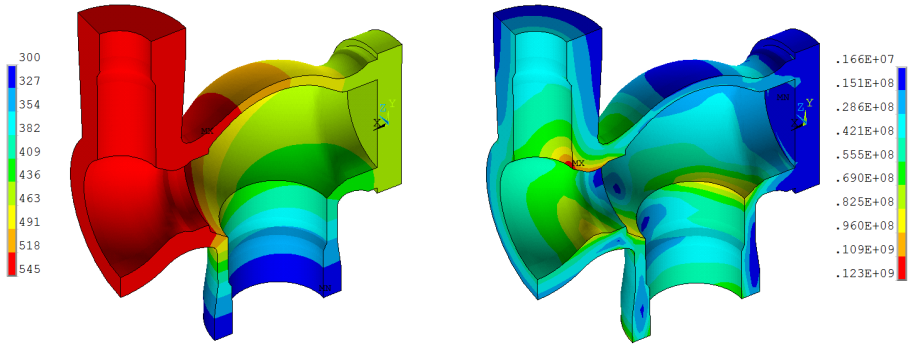

(a) (b)

Fig. 4. Steady-state (reference) valve working conditions: a) the temperature distribution in °C, b) von Mises stress distribution in Pa

by the injection of water dissipated on the inner surface of the heated valve body with the convection heat transfer coefficient $\alpha = 20000$ W/(m^{2}K), Biot number $Bi = 13.9 \div 27.8$, and the coefficient of thermal conductivity $k = 46$ W/(m·K).

2. The three-dimensional FEM analysis of elastic-plastic material deformation of the valve body wall during the heat shock cycle (Fig. 5) including calculations of low-fatigue cycle and macroscopic crack initiation on the surface. The yield stress was assumed to be $R_{02} = 260 \div 186$ MPa (in the temperature range of 20÷550°C), the kinematic strain hardening of 2÷1.88 GPa, the coefficient of thermal expansion $\lambda = 1.17 \div 1.39 \cdot 10^{-5}$ 1/K and the material constants in Manson-Coffin law were taken from the experimental results for the low-cyclic failure for mechanical loads at the level of $k = 0.52$ and $C = 0.525$.

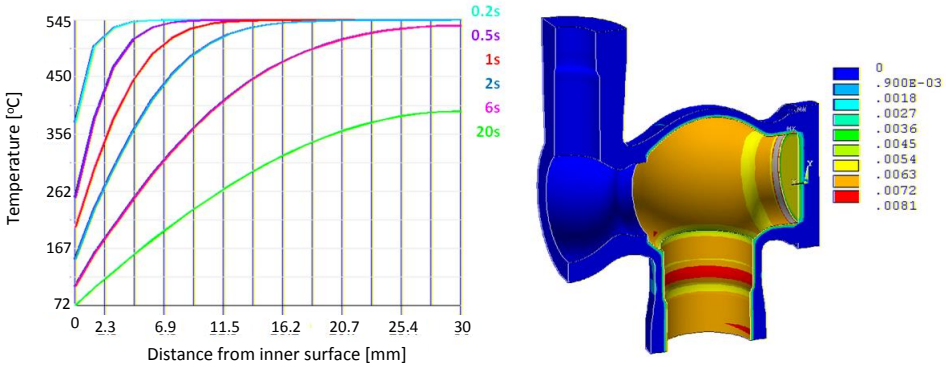

(a) (b)

Fig. 5. Heat shock caused by water injection: a) the temperature [°C] distribution across the valve wall at the time of 20 s of the injection period, b) the equivalent plastic strain in at the time $T = 4$ sec

3. The calculations of the dynamics of a the crack propagation into the body wall for the worst configuration of the fracture (axisymmetric FEM model of latitudinal crack in the spherical part of the body) and the mechanism of brittle fracture. Models of cracks were developed for the depths from 5 mm to 20 mm using elements with singularity and the elastic deformation model. The model included the change in stress intensity factor ΔK_I along the front of the crack taking into account the impact of the pressure and the transient heat transfer during the injection of water (Fig. 6). Using Erdogan-Paris law of crack development, the cracking speed was determined for each crack depth (Fig. 7).

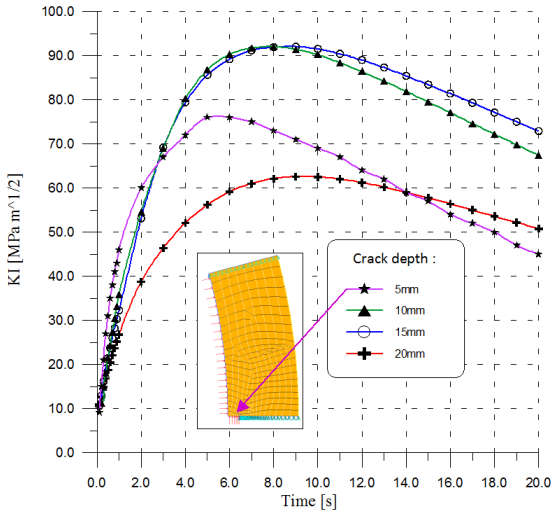

Fig. 6. Changes in the stress intensity factor K_I at the crack front for different depths of the cracks during heat shock. Axisymmetric model crack with a depth of 5mm and pressure load on its surface shown in the box

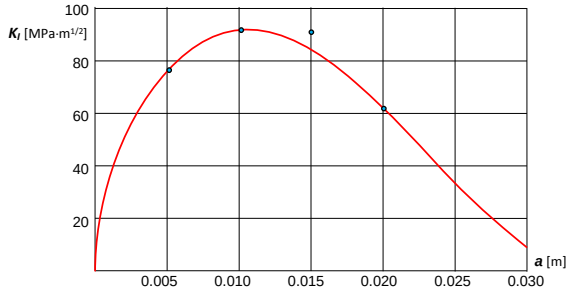

Fig. 7. The maximum of stress intensity factor K_I [MPa·m$^{1/2}$] versus crack depth in meters for thermal shock and internal pressure $p = 46$ bar approximated for four crack depths according to:

$$K_I = 200\sqrt{\frac{a}{g}}\left(1 - \left(\frac{a}{1.15g}\right)^2\left(3 - \frac{2a}{1.15g}\right)\right)$$

Based on the performed analyses, it has been found that the maximum value of the plastic strain of the spherical inner surface of the valve chamber during the thermal shock reaches $\varepsilon_{pl} = 7.2‰$ and takes place in the third second of the process. Taking into account that the subsequent cycle of heating of the inner surface is fast enough, the determined value of plastic deformation can be taken as an upper estimate for a plastic strain change at the 1 cycle load. The number of cycles of low-cyclic damage of the surface in the form of a macroscopic crack initiation calculated using Manson-Coffin equation reached $N_f = 3470$ cycles. From this point it was assumed safely that the development of a crack took place in a brittle manner according to Erdogan-Paris equation. In fact, the crack can be either plastic or mixed especially in the first phase of its growth. This hypothesis could be verified by microscopic examination of the fracture surfaces, however, no destructive testing was allowed in this case.

In the analysis of the crack development using the axisymmetric model it was assumed that the crack progressed latitudinally on inner surface of the valve body and the calculations were performed for four crack depths: 5 mm, 10 mm, 15 mm and 20 mm (Fig. 6). The conditions of transient convective heat transfer occurred only on the spherical surface, but the presence of internal pressure was also included on the surface of the cracks (Fig. 6). The variations of the stress intensity factor K_I on the crack front during the heat shock were determined to be below the material fracture toughness ($K_{IC} = 100$ MPa·m$^{1/2}$),which indicated stable crack growth. The critical crack depth a_{kr} for the average stress σ on valve wall, at the steady state conditions (Fig. 4) and crack geometry factor Q, calculated as:

$$a_{kr} = \frac{Q}{1.21\pi}\left(\frac{K_{IC}}{\sigma}\right)^2. \tag{13}$$

were over the actual valve body wall thickness, which proved the safe damage mode: “leak but not burst”.

Based on K_I time history plots (Fig. 6), the maximum values of $K_I^{\max}$ were determined and shown as a function of crack depth (Fig. 7). Assuming that during the phase of the cycle associated with heating up the body the minimum value of the stress intensity factor $K_I^{\min} = 0$, the change in stress intensity factors at one thermal cycle is $\Delta K_I = K_I^{\max}$. Thus, the crack speed is calculated as a function of the depth of the crack, and it shows the character of the cracks development due to thermal shocks and internal pressure in the valve body (Fig. 8). From the graph it can be read that growth of the crack depth from 5 mm to 15 mm requires about 700 thermal cycles, while the next 600 cycles increase its depth by approximately 5 mm. At the depth of 27 mm, the crack velocity decreases practically to zero and the crack stops to propagate.

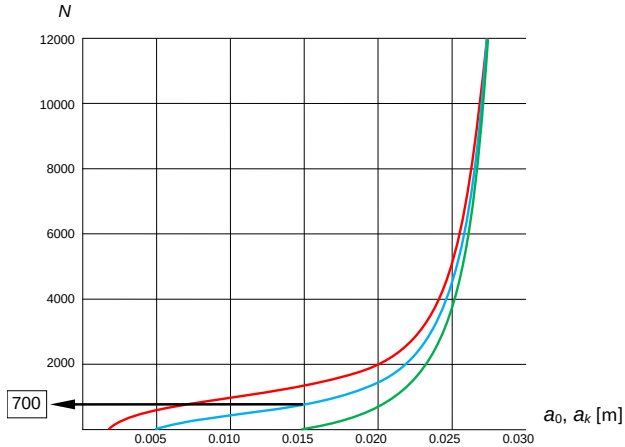

Fig. 8. Graphs of the number of load cycles N causing the increase in crack depth a_0 = 2 mm, 5 mm, 15 mm to the final depth a_k (based on the integration of the Erdogan-Paris equation for $C = 2 \cdot 10^{-8}$ mm/cycle, $m = 3$, ΔK_I from FEM calculations)

2.4. Remarks

On the basis of the calculations and analyses the following conclusions can be drawn regarding the creation and dynamics of the fatigue cracks growth caused by thermal shocks on the inner surface of the valve body.

- Thermal shocks cause sudden contraction of the inner surface layers of the valve body.
- The effect of cyclic changes of plastic strain on the inner surface of the body is the low cycle fatigue of the material that leads to the formation of fatigue cracks after approx. N = 3000–4000 cycles of thermal shocks.
- The speed of cracking in the early stages of cracks growth is increasing rapidly due to the high stress concentration at the crack tip, which is located in the zone of extreme temperature gradients.
- With the increasing crack depth, the intensity of the stresses during the subsequent thermal shocks decreases, as the crack tip moves out of the zone of high thermal gradients and differences in thermal expansion.
- Once the crack reaches the depth of approx. 25–27 mm (in the course of approx. next 4000–6000 cycles), the rate of crack growth drops to zero and the crack stops to propagate through the body wall.
- In the final state, the cracked material, when subjected to a temperature gradient during shock, compensates the differences of thermal expansion within the cracked layer of the body.
- It is likely that through-thickness wall rupture may lead to leakage, but not to burst.

The structure spontaneously adapts to extreme operating conditions.

In these analyses, the possibly most unfavorable operating conditions and the fastest possible growth of the crack were assumed. It has been found that, in reality, the process of fatigue and cracking proceeds slower, however, the determined values of the number of load cycles are in good agreement with users' observations of the valve, which indicate that the maximum crack depth of approx. 20 mm occurs after approximately 1.5 year of operation with the daily number of cooling cycles from 40 to 75. After this period, practically no further increase in the depth of cracks in the valve bodies was observed, which proves the ability of the structure to adapt to work in the vicinity of cracks, despite initial surface damage as a result low-cyclic thermo-mechanical fatigue. Of course, it is possible to protect the valve body wall from cracking of the surface by applying internal screens made of the segments of heat resistant metal sheets. This solution, which in a specific way simulates the behavior of a cracked surface, is recommended for the use in the case of a new valve.

3. The case of the turbine

The object of this analysis was a rotor of the medium-pressure section of the TK200 turbine, in which, at an occasional survey, a failure was noticed between the first and second stage (Fig. 9). In this area, a fracture appeared in the radial direction around the circumference of the rotor, which propagated into up to 40 mm. Because the turbine was in good dynamic condition (measured and verified analytically [18–20]), the damage could not be caused by a lack of balance. The cause was suspected to be of thermal nature, because according to

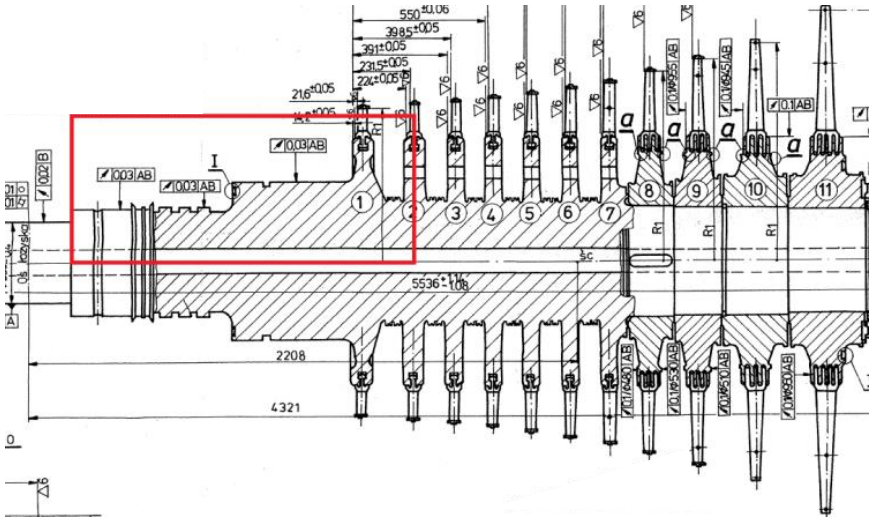

Fig. 9. Turbine TK-200 – geometry of the rotor

reports, an improper supply of bleed steam, rather than live steam, was recorded on numerous occasions (difference approx. 200°C). Introducing such a cool steam on the hot rotor causes rapid cooling and may promote the development of cracks.

It was decided to analyze the state of stress in the area between first and second stage of the rotor resulting from the cooling with a steam jet.

The geometry of the area between first and second stage of the rotor was based on the technical documentation provided (Fig. 9).

3.1. Determination of the temperature distribution during steam jet cooling of the hot turbine TK 200

The axisymmetric thermal FEM model of the rotor assembly was built using 4-noded elements. The model included the part of the turbine up to the plane of the second stage.

Initially the non-stationary heating problem was considered up to 48 hours. Heat exchange coefficients and the steam temperature applied were chosen by trial so as to obtain reliable temperature distribution (Fig. 10).

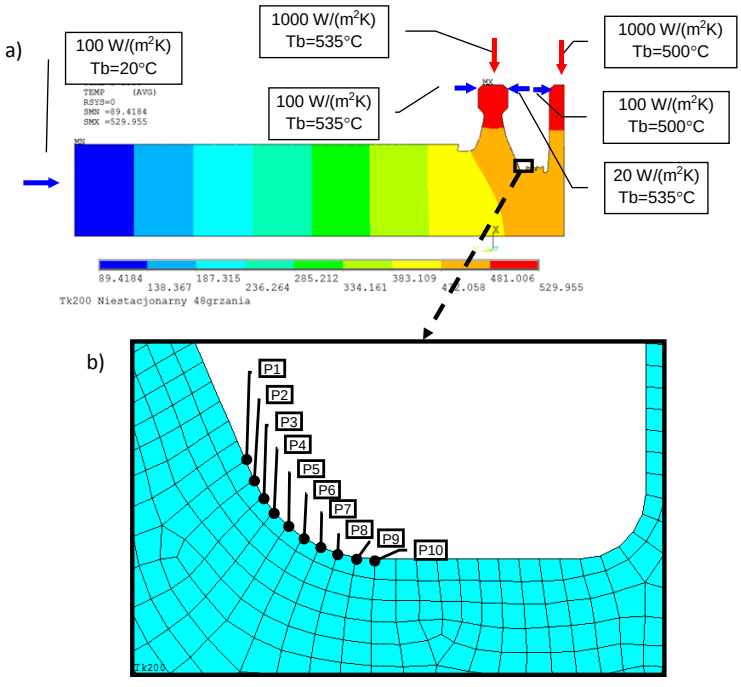

Fig. 10. FEM model of the part of the turbine rotor: a) heating parameters in the model against temperature distribution after 48 hours of heating, b) a part of the finite element mesh in the bottom of the notch indicating the job parameters monitoring points

Then evaporative cooling was applied on the surfaces of first and second stage. A constant heat transfer coefficient and a constant steam temperature were assumed. These parameters were changed in the following alternative tasks, assuming the heat exchange coefficient at the level of 200 W/(m^{2}K), and the steam temperature of 350°C and 200°C (variant less optimistic). The cooling process lasted 60 minutes and took place in 240 equal time steps (every 15 seconds).

3.2. Determination of thermal stresses during steam jet cooling of the TK 200 turbine

Based on the results of unsteady heat transfer analysis, the load steps were prepared for the structural analysis. The type of elements was switched from thermal to structural (4-noded), keeping the axisymmetric option.

Symmetry was assumed in the plane of the second stage. The quasi-static structural problem was solved using the aforementioned load steps. The problem of heating was solved in a single step, and cooling was solved in 240 quasi-static steps (every 15 seconds).

Particular attention was paid to the state of stress in the notch between first and second stage, where 10 measuring points were located at the nodes of the finite element mesh (Fig. 10b). At these points principal stress – S1 as a function of time was monitored. Representative curves of changes in the principal stresses S1 as a function of time for cooling at 200 W/(m^{2}K) and temperature of steam 350°C are shown in Fig. 11. These functions reach a maximum around 20 minutes from the start of cooling.

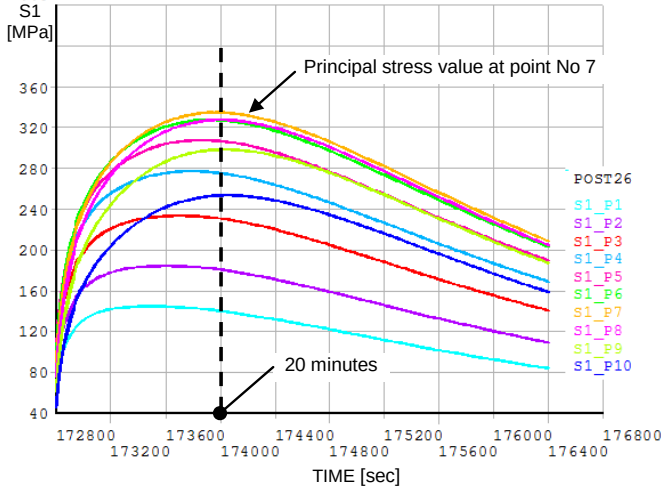

Fig. 11. Distributions of principal stress S1 [MPa] at notch points – T_{steam} = 350°C

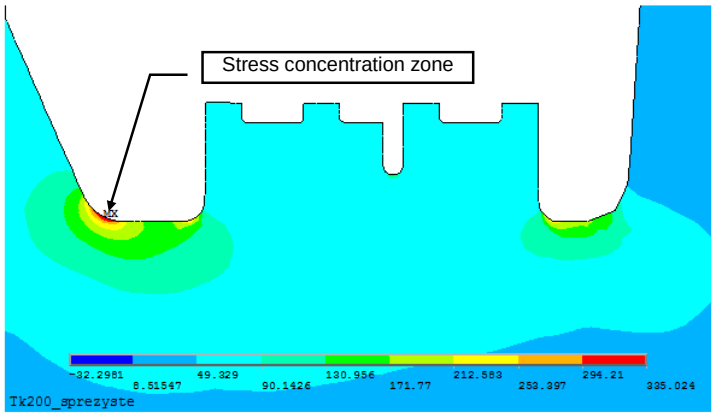

Fig. 12. Distribution of principal stress S1 [MPa] (20 minutes of cooling) – T_{steam} = 350°C

Stress concentration occurs at the point No. 7, and so this was treated as a critical point for the zone (Fig. 12) and fracture was located there.

3.3. Determination of stress intensity factors for cracks models

In the stress concentration zone (Fig. 12), a family of cracks of different depths was modelled. At the crack tip the concentration point was introduced, and the grid of 8-noded singular elements (midside nodes moved to ¼ side length) was built around to model a singularity there. An example of such a grid for crack depth of a = 6 mm is shown in Fig. 13.

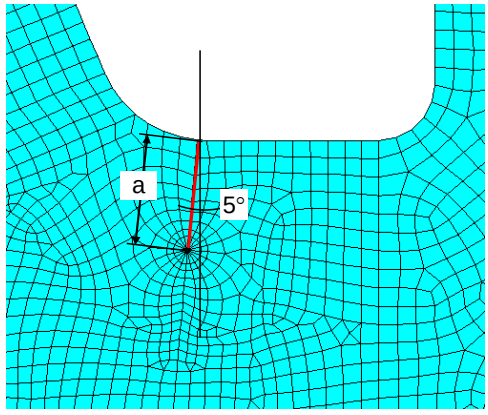

Fig. 13. The grid of elements around the crack tip (a = 6 mm)

Representative curves of changes in the principal stress (S1) and equivalent stress (SEQV) as a function of time at a crack tip node for the case a = 2 mm (cooling at 200 W/(m^{2}K) and T_{steam} = 350°C) are shown in Fig. 14. Fig. 15

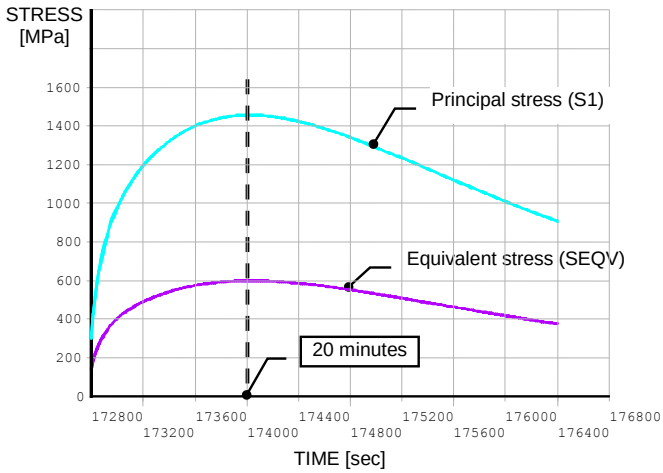

Fig. 14. Changes in S1 and SEQV in MPa stress at the crack tip (a = 2 mm). Cooling 200W/(m^{2}K) and 350°C

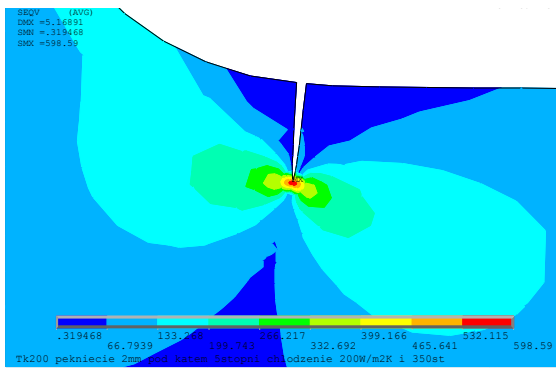

Fig. 15. Distributions of equivalent stress SEQV in MPa for crack (a = 2 mm). Cooling 200W/(m^{2}K) and 350°C– time point 20 minutes of cooling

shows an example of equivalent stress distribution at 20 minutes from the start of cooling.

For cracks with a depth of 0.5 mm to 40 mm, the stress intensity factor was determined by the crack opening displacement method (COD). Fig. 16 shows a plot of stress intensity factors for two modes of fracture K_I and K_{II} for a family of cracks upon cooling (200W/(m^{2}K) and 350°C).

For the crack depth of a = 6 mm, the effect of the cooling parameters on the stress intensity factors was examined (Fig. 17). In the case of heat transfer coefficient of 200 W/(m^{2}K), the stress intensity factor K_I decreases approximately by half if the coolant temperature is changed from 200 to 350°C.

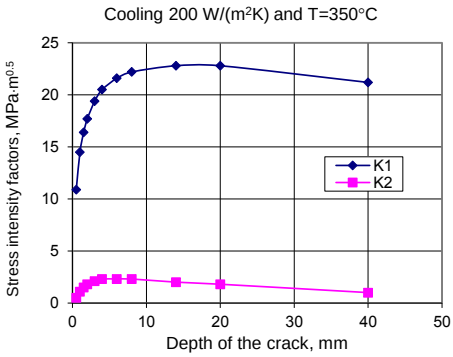

Fig. 16. Distributions of stress intensity factors K_I and K_{II} as a function of crack depth at cooling 200W/(m^{2}K) and 350°C determined at time points 20 minutes from the start of cooling

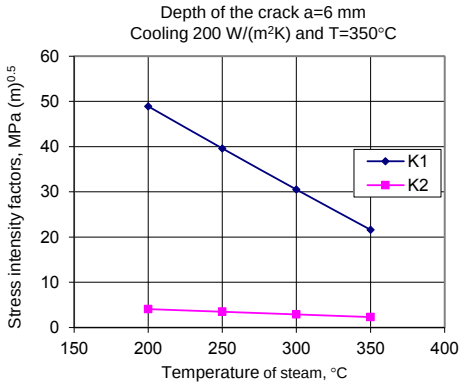

Fig. 17. Changes in stress intensity factors K_I and K_{II} as a function of the steam temperature with cooling of 200W/(m^{2}K) – for crack depth a = 6 mm, set at time points 20 minutes from the start of cooling

3.4. Estimating the number of thermal cycles for crack models

An attempt was made to estimate the number of thermal cycles using the Erdogan-Paris equation.

Assuming $C = 0.98 \cdot 10^{-8}$ mm/cycle and $m = 2.1$ [10] the crack propagation per cycle reaches $\mathrm{d}a/\mathrm{d}N = 0.98 \cdot 10^{-8}(K_I)^{2.1}$, where K_I is presented in kG/m$^{3/2}$ and we can show a variation of crack velocity as a function of the depth of the crack (Fig. 18).

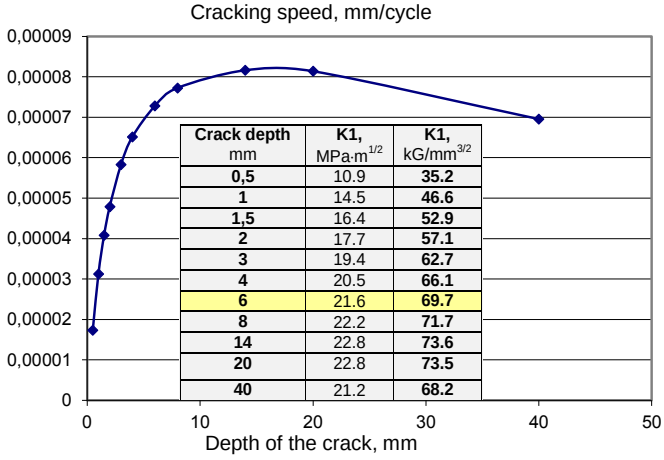

Crack depth mm	K1, MPa·m$^{1/2}$	K1, kG/mm$^{3/2}$
0,5	10.9	35.2
1	14.5	46.6
1,5	16.4	52.9
2	17.7	57.1
3	19.4	62.7
4	20.5	66.1
6	21.6	69.7
8	22.2	71.7
14	22.8	73.6
20	22.8	73.5
40	21.2	68.2

Fig. 18. Variability of cracking speed as a function of the depth of the crack (200 W/(m^{2}K) and 350°C)

Finally, integrating the inverse function of the cracking speed, onecan show the relation between the crack depth and the number of cycles. Chart of crack development from $a_0 = 0.5$ mm to $a = 40$ mm is shown in Fig. 19.

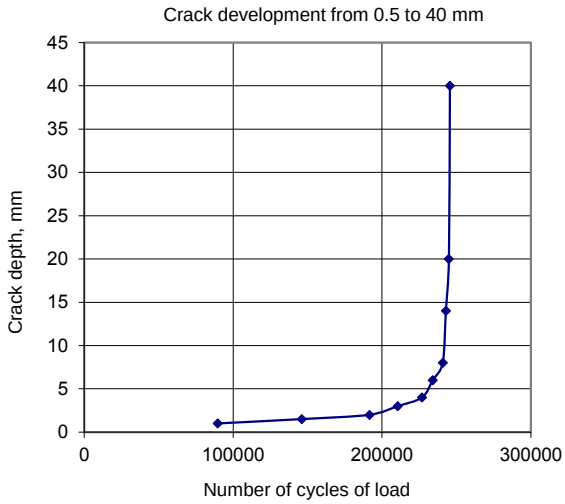

Fig. 19. Crack depth versus number of cycles (200W/(m^{2}K) and 350°C)

3.5. Comments and requests

The attempt to assess the impact of the development of cracks in the cooling conditions showed that, in the area of the notch behind the 1st stage of TK200, a local tensile stress concentration occurs (Fig. 12). This may stimulate the formation and growth of cracks.

The milder cooling scenario assumed in further calculations (200 W/(m^{2}K) and 350°C) shows that the peak stress occurs in about 20 minutes from the start of cooling (Fig. 11).

The scenario of cracks growth adopted later allowed us to estimate the stress intensity factor K_I, which reaches the highest value for the depth of the cracks in the range of 14–20 mm (Fig. 16).

For cracks with a depth of 6 mm, the change of the temperature T_{steam} from 350°C to 200°C, would result in a doubling of the value of the K_I coefficient (Fig. 17).

The attempt to assess the development of the crack as function of the number of cooling cycles (Fig. 19) from the initial value $a_0 = 0.5$ mm to $a = 40$ mm shows that the crack would reaches a length of:

– 1 mm at approx. 90 thousand cycles,
– 2 mm at approx. 192 thousand cycles,
– 4 mm at approx. 225 thousand cycles,

– 8 mm at approx. 241 thousand cycles,
– 20 mm at approx. 245 thousand cycles,
– 40 mm at approx. 246 thousand cycles.

The resulting large number of cycles indicates that the cooling cycles that occur rarely cannot be the cause of cracking.

4. Final conclusions

Low-cyclic fatigue and subsequent crack growth on steam system HP devices under thermal shocks appears to be often the reason for structural failure. The destructive effects of heat shock occur quite soon for large Biot number and the abrupt change of heat transfer on the surface, which can be seen e.g. at the rapid evaporation of the liquid (case of the valve body). Gases generally do not cause such dramatic effects (the case of turbine rotor shaft). However, after initial quick rise of material fatigue and damage due to crack propagation, dynamics of the process usually slows down as the result of lower temperature gradients deep inside the element and compensation of thermal expansions by cracked surface. Consequently, cracking speed drops to zero, and further cracking stops before reaching the critical depth. The phenomena of structural accommodation to the destructive fatigue loads occurs for the processes which are controlled by displacements rather than forces. The redistribution of stresses due to the destructive form of non-linear behavior of the material (creep, cracking) after a certain time or finite number of initial cycles of load (particularly the kinematic excitations or dominated by them complex loads) often enables safe, long-term operation of the structure as a result of adaptation to a given load scheme. In each case of cracking, a calculation of the critical crack depth helps to evaluate possible consequences of structural damage.

Acknowledgements

This work was supported by Polish National Centre for Research and Development NCBR) POIG project 1.3.1-14-074 / 12 task 4.

Manuscript received by Editorial Board, December 07, 2015;
final version, June 03, 2016.

References

[1] M. Malesa, K. Malowany, J. Pawlicki, M. Kujawinska, P. Skrzypczak, A. Piekarczuk, T. Lusa, and A. Zagorski. Non-destructive testing of industrial structures with the use of multi-camera Digital Image Correlation method. *Engineering Failure Analysis*, 2016. doi: 10.1016/j.engfailanal.2016.02.002.

[2] J.A. König. *Shakedown of elastic-plastic structures*, volume 7. Elsevier, 2012.

[3] S. Pycko. Variable loading and imposed displacements in the shakedown theory. *IFTR Reports*, 1993.

[4] T.J. Lu and N.A. Fleck. The thermal shock resistance of solids. *Acta materialia*, 46(13):4755–4768, 1998.

[5] Z. Zwoliński and Bielawski G. Optimizational approach to the elasto-plastic analysis. In *Abstr, I European Solid Mech. Conf. Munich*, 1991.

[6] A. Weroński. *Zmęczenie cieplne metali (Thermal fatigue of metals)*. WNT (Scientific-Technical Publishers), Warszawa, 1983. (in Polish).

[7] Z. Orłoś. *Naprężenia cieplne (Thermal stress)*. PWN (Polish Scientific Publishers), Warszawa, 1991. (in Polish).

[8] S. Wiśniewski and T.S. Wiśniewski. *Wymiana ciepła (Heat exchange)*. WNT (Scientific-Technical Publishers), Warszawa, 1994. (in Polish).

[9] S. Kocańda and A. Kocańda. *Niskocyklowa wytrzymałość zmęczeniowa metali (Low cycle fatigue strength of metals)*. PWN (Polish Scientific Publishers), Warszawa, 1989. (in Polish).

[10] S. Kocańda. *Zmęczeniowe niszczenie metali (Fatigue destruction of metals)*. WNT (Scientific-Technical Publishers), Warszawa, 1978. (in Polish).

[11] M.H. Aliabadi and D.P. Rooke. *Numerical fracture mechanics*, volume 8. Springer Science & Business Media, 1991.

[12] C.R.F. Azevedo and A. Sinátora. Erosion-fatigue of steam turbine blades. *Engineering Failure Analysis*, 16(7):2290–2303, 2009.

[13] A.Z. Rashid, J. Purbolaksono, A. Ahmad, and S.A. Ahmad. Thermal fatigue analysis on cracked plenum barrier plate of open-cycle gas turbine frame. *Engineering Failure Analysis*, 17(2):579–586, 2010.

[14] F. Szmytka, M. Salem, F. Rézaï-Aria, and A. Oudin. Thermal fatigue analysis of automotive diesel piston: Experimental procedure and numerical protocol. *International Journal of Fatigue*, 73:48–57, 2015.

[15] X. Su, M. Zubeck, J. Lasecki, C.C. Engler-Pinto, C. Tang, H. Sehitoglu, and J. Allison. Thermal fatigue analysis of cast aluminum cylinder heads. SAE Technical Paper 2002-01-0657, 2002. doi: 10.4271/2002-01-0657.

[16] W. Wunderlich and M. Hayashi. Thermal cyclic fatigue analysis of three aluminum piston alloys. *International Journal of Material and Mechanical Engineering*, (1):57–60, 2012.

[17] G. Krzesiński, T. Zagrajek, P. Marek, and P. Borkowski. *Metoda elementów skończonych w mechanice materiałów i konstrukcji. Rozwiązywanie wybranych zagadnień za pomocą systemu ANSYS (Finite element method in mechanics of materials and structures. Solving some problems with ANSYS system)*. Oficyna Wydawnicza Politechnki Warszawskiej (Publishing House of Warsaw University of Technology), 2015. (in Polish).

[18] T. Zagrajek, G. Krzesiński, J. Pawlicki, J. Zwoliński, F. Dul, P. Marek, D. Głowacki, P. Borkowski, K. Rogowski, P. Wymysłowski, K. Kozakiewicz, B. Dec, K. Draszyński, and M. Żak. *Monitorowanie zużycia eksploatacyjnego i optymalizacja procesu naprawczego wirników turbin parowych (Monitoring wear and tear and optimize the process of repair of steam turbine rotors)*. Sprawozdanie z wykonania prac analityczno-modelowych projektu POIG 1.3.1-14.074/12 (Report on the implementation of analytical and modeling project), 2013. (in Polish).

[19] F. Dul and J. Pawlicki. Modeling of hydrodynamic bearing oil film properties for power turbine rotordynamics prediction. *Journal of Power Technologies*, 2017. (Submitted for publication).

[20] P. Borkowski, D. Głowacki, A. Nowakowska, J. Pawlicki, and J. Zwoliński. FE analysis of a steam turbine HP rotor blade stage concerning material effort, dynamic properties and creep damage assessment. *Archive of Mechanical Engineering*, 63(1):163–185, 2016.

Analiza rozwoju pęknięć w elementach urządzeń energetyki cieplnej pracujących w warunkach zmiennych temperatur

S t r e s z c z e n i e

W pracy przedstawiono szczegółową analizę rozwoju pęknięć w wyniku niskocyklicznego zmęczenia materiału w warunkach szoków cieplnych i oddziaływania ustalonych obciążeń statycznych. Przeprowadzono analizę przebiegu procesu pękania na przykładzie korpusu zaworu redukcyjnego pary w elektrowni węglowej i wału wirnika turbiny parowej. Głównym czynnikiem w obydwu przypadkach są mniej lub bardziej gwałtowne powtarzalne cykle zmian temperatury. W przypadku inicjacji pęknięcia po stosunkowo małej liczbie cykli zmian obciążenia mechanizm zmęczenia zależy od naprzemiennej lub naprzemienno-przyrostowej zmiany odkształceń plastycznych. Propagację pęknięcia w głąb materiału wyznaczono metodami klasycznej mechaniki pękania na podstawie modeli MES i najbardziej niebezpiecznego modelu pękania kruchego. Przedstawiono przypadek przystosowania się konstrukcji do pracy w warunkach szoków cieplnych i pękania.